Chapter 2

Physical Chemistry of Solid Surfaces

2.1. Introduction

Nanostructures and nanomaterials possess a large fraction of surface atoms per unit volume. The ratio of surface atoms to interior atoms changes dramatically if one successively divides a macroscopic object into smaller parts. For example, for a cube of iron of 1 cm^3, the percentage of surface atoms would be only 10^{-5}%. When the cube is divided into smaller cubes with an edge of 10 nm, the percentage of the surface atoms would increase to 10%. In a cube of iron of 1 nm^3, every atom would be a surface atom. Figure 2.1 shows the percentage of surface atoms changes with the palladium cluster diameter.[1] Such a dramatic increase in the ratio of surface atoms to interior atoms in nanostructures and nanomaterials might illustrate why changes in the size range of nanometers are expected to lead to great changes in the physical and chemical properties of the materials.

The total surface energy increases with the overall surface area, which is in turn strongly dependent on the dimension of material. Table 2.1 listed how the specific surface area and total surface energy of 1 g of sodium chloride vary with particle size.[2] The calculation was done based on the following assumptions: surface energy of 2×10^{-5} J/cm^2 and edge energy of 3×10^{-13} J/cm, and the original 1 g cube was successively divided into smaller cubes. It should be noted that the specific surface area and, thus, the total surface energy are negligible when cubes are large, but become significant for very small particles. When the particles change from centimeter size to nanometer size, the surface area and the surface energy increase seven orders of magnitude.

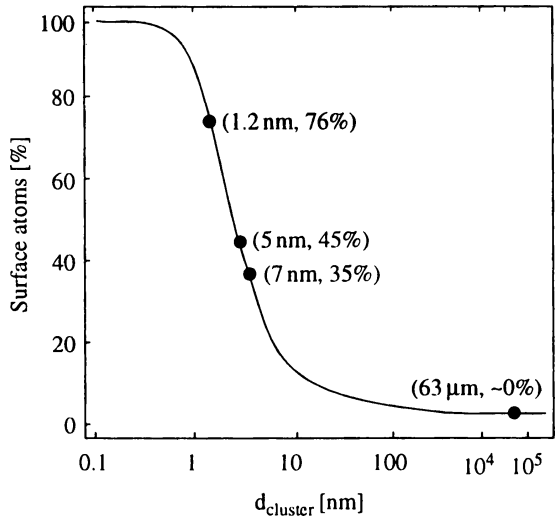

Figure 2.1. The percentage of surface atoms changes with the palladium cluster diameter. [C. Nützenadel, A. Züttel, D. Chartouni, G. Schmid, and L. Schlapbach, *Eur. Phys. J.* **D8**, 245 (2000).]

Table 2.1. Variation of surface energy with particle size.[2]

Side (cm)	Total Surface Area (cm^2)	Total Edge (cm)	Surface Energy (J/g)	Edge Energy (J/g)
0.77	3.6	9.3	7.2×10^{-5}	2.8×10^{-12}
0.1	28	550	5.6×10^{-4}	1.7×10^{-10}
0.01	280	5.5×10^{4}	5.6×10^{-3}	1.7×10^{-8}
0.001	2.8×10^{3}	5.5×10^{6}	5.6×10^{-2}	1.7×10^{-6}
10^{-4} (1 μm)	2.8×10^{4}	5.5×10^{8}	0.56	1.7×10^{-4}
10^{-7} (1 nm)	2.8×10^{7}	5.5×10^{14}	560	170

Due to the huge surface area, all nanostructured materials possess a huge surface energy and, thus, are thermodynamically unstable or metastable. One of the great challenges in fabrication and processing of nanomaterials is to overcome the surface energy, and to prevent the nanostructures or nanomaterials from growth in size, driven by the reduction of overall surface energy. In order to produce and stabilize nanostructures and nanomaterials, it is essential to have a good understanding of surface

energy and surface physical chemistry of solid surfaces. In this chapter, the origin of the surface energy will be reviewed first, followed with detailed discussion of the possible mechanisms for a system or material to reduce the overall surface energy. Then the attention will be focused on the chemical potentials as a function of surface curvature and its implications. Finally, two mechanisms to prevent the agglomeration of nanomaterials will be discussed.

2.2. Surface Energy

Atoms or molecules on a solid surface possess fewer nearest neighbors or coordination numbers, and thus have dangling or unsatisfied bonds exposed to the surface. Because of the dangling bonds on the surface, surface atoms or molecules are under an inwardly directed force and the bond distance between the surface atoms or molecules and the subsurface atoms or molecules, is smaller than that between interior atoms or molecules. When solid particle are very small, such a decrease in bond length between the surface atoms and interior atoms becomes significant and the lattice constants of the entire solid particles show an appreciable reduction.[3] The extra energy possessed by the surface atoms is described as surface energy, surface free energy, or surface tension. Surface energy, γ, by definition, is the energy required to create a unit area of "new" surface:

$$\gamma = \left(\frac{\partial G}{\partial A} \right)_{ni,T,P}, \tag{2.1}$$

where A is the surface area. Let us consider separating a rectangular solid material into two pieces as illustrated in Fig. 2.2. On the newly created surfaces, each atom is located in an asymmetric environment and will move towards the interior due to breaking of bonds at the surface. An extra force is required to pull the surface atoms back to its original position. Such surface is ideal and also called singular surface. For each atom on such a singular surface, the energy required to get it back to its original position will be equal to the number of broken bonds, N_b, multiplying half of the bond strength, ε. Therefore, the surface energy is given by:

$$\gamma = \left(\frac{1}{2} \right) N_b \varepsilon \rho_a, \tag{2.2}$$

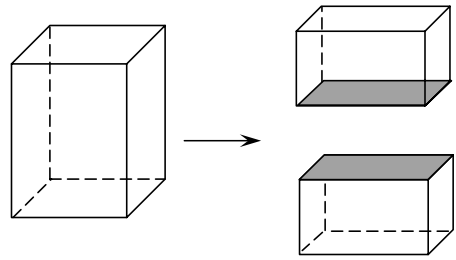

Figure 2.2. Schematic showing two new surfaces being created by breaking a rectangular into two pieces.

where ρ_a is the surface atomic density, the number of atoms per unit area in the new surface. This crude model ignores interactions owing to higher order neighbors, assumes that the value of ε is the same for surface and bulk atoms, and does not include entropic or pressure–volume contributions. This relation only gives a rough estimation of the true surface energy of a solid surface, and is only applicable to solids with rigid structure where no surface relaxation occurs. When there is an appreciable surface relaxation, such as the surface atoms moving inwardly, or there is a surface restructuring, surface energy will be lower than that estimated by the above equation. In spite of the overly simplified assumptions used in Eq. (2.2), it does provide some general guidance. Let us take an elemental crystal with a face-centered cubic (FCC) structure having a lattice constant of *a*, as an example to illustrate the surface energy on various facets. Each atom in such a FCC crystal has a coordination number of 12. Each surface atom on {100} facets would have four broken chemical bonds, and the surface energy of {100} surface can be calculated using Eq. (2.2) and Fig. 2.3(a):

$$\gamma_{\{100\}} = \left(\frac{1}{2}\right)\left(\frac{2}{a^2}\right)4\varepsilon = \frac{4\varepsilon}{a^2}. \tag{2.3}$$

Similarly, each atom on {110} surface has five broken chemical bonds and {111} has three. The surface energies of {110} and {111} surfaces are given, calculating from Figs. 2.3(b) and 2.3(c):

$$\gamma_{\{110\}} = \frac{5}{\sqrt{2}}\frac{\varepsilon}{a^2}, \tag{2.4}$$

$$\gamma_{\{111\}} = \frac{2}{\sqrt{3}}\frac{\varepsilon}{a^2}. \tag{2.5}$$

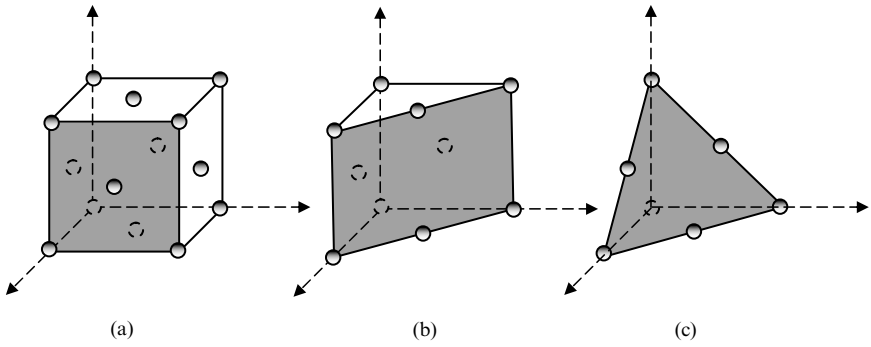

Figure 2.3. Schematic representing low index faces of a face-centered cubic (FCC) crystal structure: (a) {100}, (b) {110}, and (c) {111}.

The readers can easily figure out the fact that low index facets have low surface energy according to Eq. (2.2). Thermodynamics tells us that any materials or systems are stable only when they are in a state with the lowest Gibbs free energy. Therefore, there is a strong tendency for a solid or a liquid to minimize their total surface energy. There are a variety of mechanisms to reduce the overall surface energy. The various mechanisms can be grouped into atomic or surface level, individual structures, and the overall system.

For a given surface with a fixed surface area, the surface energy can be reduced through (1) surface relaxation, the surface atoms or ions shift inwardly which occur more readily in liquid phase than in solid surface due to rigid structure in solids, (2) surface restructuring through combining surface dangling bonds into strained new chemical bonds, (3) surface adsorption through chemical or physical adsorption of terminal chemical species onto the surface by forming chemical bonds or weak attraction forces such as electrostatic or van der Waals forces, and (4) composition segregation or impurity enrichment on the surface through solid-state diffusion.

Let us take the surface atoms on an atomic flat {100} surface as an example, assuming the crystal has a simple cubic structure and each atom has a coordination number of six. The surface atoms are linked with one atom directly beneath and four other surrounding surface atoms. It is

reasonable to consider each chemical bond acting as an attractive force; all the surface atoms are under the influence of a net force pointing inwardly and perpendicular to the surface. Understandably, under such a force, the distance between the surface atomic layer and the subsurface atomic layer would be smaller than that inside the bulk, though the structure of the surface atomic layer remains unchanged. In addition, the distance between the atomic layers under the surface would also be reduced. Such surface relaxation has been well-established.[4–7] Furthermore, the surface atoms may also shift laterally relative to the subsurface atomic layer. Figure 2.4 schematically depicts such surface atomic shift or relaxation. For bulk materials, such a reduction in the lattice dimension is too small to exhibit any appreciable influence on the overall crystal lattice constant and, therefore, can be ignored. However, such an inward or lateral shift of surface atoms would result in a reduction of the surface energy. Such a surface relaxation becomes more pronounced in less rigid crystals, and can result in a noticeable reduction of bond length in nanoparticles.[3]

If a surface atom has more than one broken bonds, surface restructuring is a possible mechanism to reduce the surface energy.[8–11] The broken bonds from neighboring surface atoms combine to form a highly strained bond. For example, such surface restructuring is found in the {111} surface of silicon crystals.[12] Surface energy of {100} faces in diamond and silicon crystals is higher than both {111} and {110} faces. However, restructured {100} faces have the lowest surface energy among three low indices faces,[13–15] and such surface restructuring can have a significant impact on the crystal growth.[16–19] Figure 2.5 shows the original {100} surface and (2 × 1) restructured {100} surface of diamond crystal.

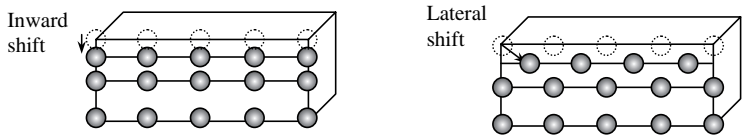

Figure 2.4. Schematic showing surface atoms shifting either inwardly or laterally so as to reduce the surface energy.

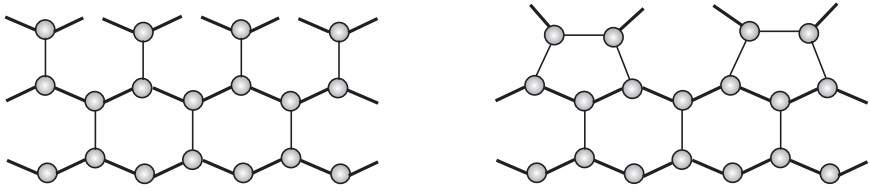

Figure 2.5. Schematic illustrating the (2 × 1) restructure of silicon (001) surface.

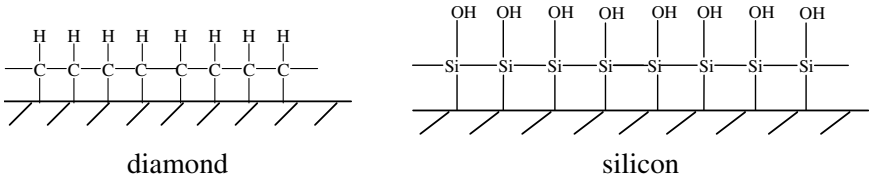

Figure 2.6. Schematic showing the surface of diamond is covered with hydrogen and that of silicon is covered with hydroxyl groups through chemisorption.

Another way to reduce the surface energy is chemical and physical adsorption on solid surfaces, which can effectively lower the surface energy.[20–23] For example, the surface of diamond is terminated with hydrogen and that of silicon is covered with hydroxyl groups as schematically shown in Fig. 2.6. These are considered as chemical adsorption. Yet another approach to reduce the surface energy is composition segregation or enrichment of impurities on the surfaces. Although composition segregation, such as enrichment of surfactants on the surface of a liquid is an effective way to reduce the surface energy, it is not common in solid surface. In bulk solids, composition segregation is not significant, since the activation energy required for solid-state diffusion is high and the diffusion distance is large. In nanostructures and nanomaterials, however, phase segregation may play a significant role in the reduction of surface energy, considering the great impact of surface energy and the short diffusion distance. Although there is no direct experimental evidence to show the impact of composition segregation on the reduction of surface energy in nanostructured materials, the difficulty in doping nanomaterials

and the ease in getting near perfect crystal structure in nanomaterials are indicative that the impurities and defects are readily to be repelled from the interior to the surface of nanostructures and nanomaterials.

At the individual nanostructure level, there are two approaches to the reduction of the total surface energy. One is to reduce the overall surface area, assuming the material is entirely isotropic. Water on a hydrophobic surface always balls up and forms a spherical droplet in free form to minimize the overall surface area. The same is also found for a glass. When heating a piece of glass to temperatures above its glass transition point, sharp corners will round up. For liquid and amorphous solid, they have isotropic microstructure and, thus, isotropic surface energy. For such materials, reduction of the overall surface area is the way to reduce the overall surface energy. However, for a crystalline solid, different crystal facets possess different surface energy. Therefore, a crystalline particle normally forms facets, instead of having a spherical shape, which in general possesses a surface energy higher than a faceted particle. The thermodynamically equilibrium shape of a given crystal can be determined by considering the surface energies of all facets, since there is a minimal surface energy when a group of surfaces is combined in a certain pattern.

In spite of the overly simplified assumptions used in the derivation of Eq. (2.2), one can use it to estimate the surface energy of various facets of a given crystal. For example, {111} surfaces in a monatomic FCC crystal have the lowest surface energy, followed by {110} and {100}. It is also easy to find that crystal surfaces with low Miller indices in general have a lower surface energy than that with high Miller indices. It does explain why a crystal is often surrounded by low index surfaces. Figure 2.7 gives some typical images of crystals with equilibrium facets.

Wulff plot is often used to determine the shape or the surfaces of an equilibrium crystal.[24,25] For an equilibrium crystal, i.e., the total surface energy reaches minimum, there exists a point in the interior such that its perpendicular distance, h_i, from the ith face is proportional to the surface energy, γ_i:

$$\gamma_i = Ch_i, \tag{2.6}$$

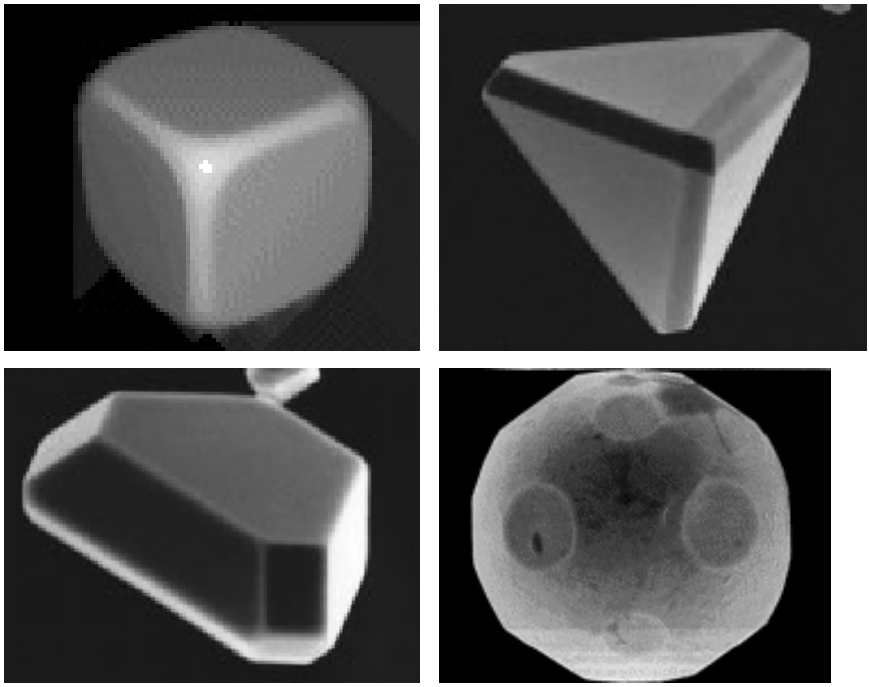

Figure 2.7. Examples of single crystals with thermodynamic equilibrium shape. Top-left: sodium chloride, top-right: silver, bottom-left: silver, and bottom-right: gold. Gold particles are formed at 1000°C and some facets have gone through roughening transition.

where C is a constant. For a given crystal, C is the same for all the surfaces. A Wulff plot can be constructed with the following steps:

(1) Given a set of surface energies for the various crystal faces, draw a set of vectors from a common point of length proportional to the surface energy and direction normal to that the crystal face
(2) Construct the set of faces normal to each vectors and positioned at its end, and
(3) Find a geometric figure whose sides are made up entirely from a particular set of such faces that do not interest any of the other planes.

Figure 2.8 gives a conformation for a hypothetical two-dimensional crystal to illustrate how the equilibrium shape of a crystal is obtained using the Wulff construction described above.[2] It should be reemphasized

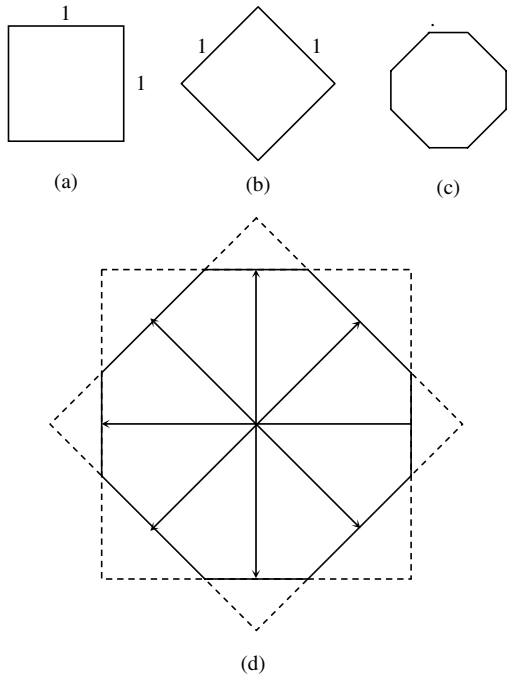

Figure 2.8. Conformation for a hypothetical two-dimensional crystal. (a) (10) plane, (b) (11) plane, (c) shape given by the Wulff construction, and (d) Wulff construction considering only (10) and (11) planes. [A.W. Adamson and A.P. Gast, *Physical Chemistry of Surfaces*, 6th edn., John Wiley and Sons, New York, 1997.]

that the geometric figure determined by the Wulff plot represents the ideal situation, i.e., the crystal reaches the minimal surface energy level thermodynamically. In practice, however, the geometric figure of a crystal is also determined by kinetic factors, which in turn are dependent on the processing or crystal growth conditions. The kinetic factors explain the fact that for the same crystal, different morphologies are obtained when the processing conditions are changed.[26]

Furthermore, it should be noted that not all crystals grown under equilibrium conditions form equilibrium facets as predicted by Wulff plots. The equilibrium crystal surfaces may not be smooth and difference in surface energy of various crystal facets may disappear.[27] Such a transition is called surface roughening or roughening transition. Below roughening temperature, a crystal is faceted. Above the roughening temperature, the

thermal motion predominates and the difference in surface energy among various crystal facets becomes negligible. As a result, a crystal does not form facets above the roughening temperature. Such a physical property can be understood by considering such a solid surface above the roughening temperature as a liquid surface.[28] Crystals grown at temperatures above the surface roughening temperature do not form facets. Examples include silicon crystals grown by Czochraski method.[29,30] Kinetic factors may also prevent the formation of facets. As will be seen in the next chapter, most nanoparticles grown by solution methods at elevated temperatures are spherical in shape and do not form any facets.

At the overall system level, mechanisms for the reduction of overall surface energy include (1) combining individual nanostructures together to form large structures so as to reduce the overall surface area, if large enough activation is available for such a process to proceed, and (2) agglomeration of individual nanostructures without altering the individual nanostructures. Specific mechanisms of combining individual nanostructures into large structures include (1) sintering, in which individual structures merge together and (2) Ostwald ripening, in which relatively large structures grow at the expense of small ones. In general, sintering is negligible at low temperatures including room temperature, and becomes important only when materials are heated to elevated temperatures, typically 70% of the melting point of the material in question. Ostwald ripening occurs at a wide range of temperatures, and proceeds at relatively low temperatures when nanostructures are dispersed and have an appreciable solubility in a solvent.

Sintering is a process that must be prevented in the fabrication and processing of nanomaterials. Fortunately, sintering becomes significant only at high temperatures. However, considering the small dimensions of nanomaterials and, thus, the extremely high surface energy, sintering can become a serious issue when nanomaterials are brought to moderate temperatures. Sintering is a complex process and involves solid-state diffusion, evaporation-condensation or dissolution-precipitation, viscous flow, and dislocation creep. Solid-state diffusion can be further divided into three categories: surface diffusion, volume diffusion, and cross grain-boundary diffusion. Surface diffusion requires the smallest activation energy, and thus is a predominant process at relatively low temperatures, whereas cross grain boundary diffusion demands the

highest activation energy and, thus, becomes significant only at high temperatures. At moderate temperatures, volume diffusion dominates the sintering process, resulting in densification and removal of pores in bulk materials. Although three solid-state diffusion processes result in markedly different microstructures, they all result in a reduction of overall surface or interface energy. Evaporation-condensation is important when nanomaterials have an appreciable vapor pressure at the processing temperature. Dissolution-precipitation occurs when the solid is dispersed in a liquid in which solid is partially soluble. Viscous flow occurs when the material is amorphous and the temperature is above the glass transition point. Creep dislocation is important particularly when material is under a mechanical stress. To preserve nanostructures during the synthesis and processing of nanomaterials and for various practical applications of nanomaterials, sintering must be avoided. A variety of mechanisms have been explored to promote sintering by the ceramic and powder metallurgy research community. A simple reverse engineering of sintering process may offer many possible approaches to prevent nanomaterials from sintering. For detailed discussion and further information on sintering, the readers are suggested to consult ceramic processing and powder metallurgy books.[31–33]

In general, sintering can be considered as a process to replace solid–vapor surface by solid–solid interface through reshaping the nanostructures in such a way that individual nanostructures are packed such that there is no gap among solid nanostructures. Ostwald ripening takes a radically different approach, in which two individual nanostructures become a single one. The large one grows at the expense of the small one until the latter disappears completely. Details of Ostwald ripening will be discussed further in the next section. The product of sintering is a polycrystalline material, whereas Ostwald ripening results in a single uniform structure. Figure 2.9 shows schematically the two different processes, though the results of both processes are similar, i.e., a reduction of total surface energy. Macroscopically, the reduction of total surface energy is the driving force for both sintering and Ostwald ripening. Microscopically, the differential surface energy of surfaces with different surface curvature is the true driving force for the mass transport during sintering or Ostwald ripening. In the next section,

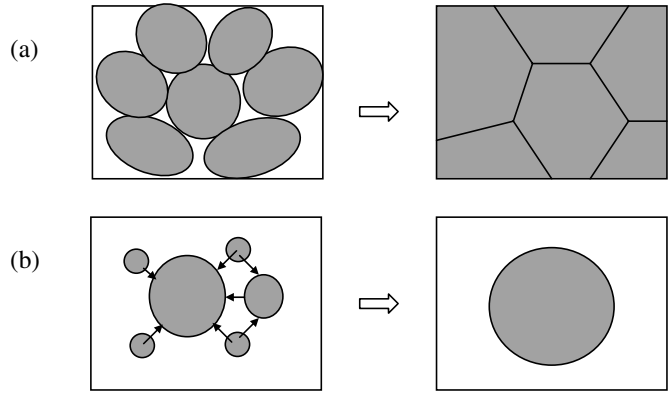

Figure 2.9. Schematic showing sintering and Ostwald ripening processes. (a) Sintering is to combine individual particles to a bulk with solid interfaces to connect each other. (b) Ostwald ripening is to merge smaller particles into a larger particle. Both processes reduce the solid–gas surface area.

we will discuss the dependence of chemical potential on the surface curvature.

In addition to combining the individual nanostructures together to form large structures through sintering or Ostwald ripening, agglomeration is another way to reduce the overall surface energy. In agglomerates, many nanostructures are associated with one another through chemical bonds and physical attraction forces at interfaces. Once formed, agglomerates are very difficult to destroy. The smaller the individual nanostructures are, the stronger they are associated with one another, and the more difficult to separate. For practical applications of nanomaterials, the formation of agglomerates should be prevented. Later in this chapter, two common methods of preventing the formation of agglomerates are discussed in detail.

So far, we have discussed the origin of surface energy and various possible mechanisms for a system to minimize its overall surface energy. In the next section, we will discuss the influences of surface curvature on surface energy. It will become clear that for a given material, concave surfaces have much lower surface energy than convex surfaces. Such differences are reflected in their respective equilibrium vapor pressure and solubility, and thus their stabilities.

2.3. Chemical Potential as a Function of Surface Curvature

As discussed in previous sections, the properties of surface atoms or molecules are different from that of interior atoms or molecules, due to their fewer bonds linking to their nearest neighbor atoms or molecules as compared with their interior counterparty. Further, the chemical potential is also dependent on the radius of curvature of a surface. To understand the relationship between chemical potential and surface curvature, let us consider transferring material from an infinite flat surface to a spherical solid particle as illustrated by Fig. 2.10. As a result of transferring of *dn* atoms from a flat solid surface to a particle with a radius of *R*, the volume change of spherical particle, *dV*, is equal to the atomic volume, Ω, times *dn*, that is:

$$dV = 4\pi R^2 dR = \Omega dn\,. \tag{2.7}$$

The work per atom transferred, $\Delta\mu$, equals to the change of chemical potential, is given by:

$$\Delta\mu = \mu_c - \mu_\infty = \gamma \frac{dA}{dn} = \frac{\gamma 8\pi R dR\,\Omega}{dV}. \tag{2.8}$$

Combining with Eq. (2.7),

$$\Delta\mu = \frac{2\gamma\Omega}{R}. \tag{2.9}$$

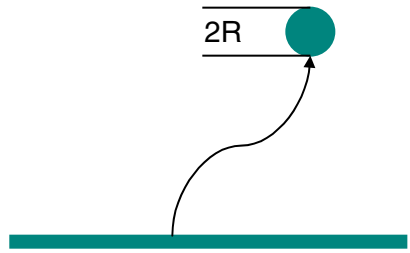

Figure 2.10. Transport of *n* atoms from the flat surface of a semi-infinite reference solid to the curved surface of a solid sphere.

This equation is also known as Young–Laplace equation, and describes the chemical potential of an atom in a spherical surface with respect to a flat reference surface. This equation can be readily generalized for any type of curved surfaces. It is known[34] that any curved surface can be described by two principle radii of curvature, R_1 and R_2, so we have:

$$\Delta\mu = \gamma\Omega\,(R_1^{-1} + R_2^{-1}). \tag{2.10}$$

For a convex surface, the curvature is positive, and thus the chemical potential of an atom on such a surface is higher than that on a flat surface. Mass transfer from a flat surface to a convex surface results in an increase in surface chemical potential. It is obvious that when mass is transferred from a flat surface to a concave surface, the chemical potential decreases. Thermodynamically, an atom on a convex surface possesses the highest chemical potential, whereas an atom on a concave surface has the lowest chemical potential. Such a relationship is also reflected by the difference in vapor pressure and solubility of a solid. Assuming the vapor of solid phase obeys the ideal gas law, for the flat surface one can easily arrive at:

$$\mu_v - \mu_\infty = -kT\ln P_\infty, \tag{2.11}$$

where μ_v is the chemical potential of a vapor atom, μ_∞, the chemical potential of an atom on the flat surface, k, the Boltzmann constant, P_∞, the equilibrium vapor pressure of flat solid surface, and T, temperature. Similarly, for a curved surface we have:

$$\mu_v - \mu_c = -kT\ln P_c, \tag{2.12}$$

where μ_c, the chemical potential of an atom on the curved surface, and P_c, the equilibrium vapor pressure of the curved solid surface. Combining Eqs. (2.11) and (2.12), we have:

$$\mu_c - \mu_\infty = \Delta\mu = kT\ln\left(\frac{P_c}{P_\infty}\right). \tag{2.13}$$

Combining with Eq. (2.10) and rearranging it, we have:

$$\ln\left(\frac{P_c}{P_\infty}\right) = \frac{\gamma\Omega(R_1^{-1} + R_2^{-1})}{kT}. \tag{2.14}$$

For a spherical particle, the above equation can be simplified as:

$$\ln\left(\frac{P_c}{P_\infty}\right)=\frac{2\gamma\Omega}{kRT}. \tag{2.15}$$

The above equation is also generally and commonly referred to as the Kevin equation and verified experimentally.[35,36] The same relation can be derived for the dependence of the solubility on surface curvature:

$$\ln\left(\frac{S_c}{S_\infty}\right)=\frac{\gamma\Omega(R_1^{-1}+R_2^{-1})}{kT}, \tag{2.16}$$

where S_c is the solubility of a curved solid surface, S_∞ is the solubility of a flat surface. This equation is also known as the Gibbs–Thompson relation.[37] Figure 2.11 shows the dependence of solubility of silica as a function of surface curvature.[38] The vapor pressure of small particles is notably higher than that of the bulk material[39–42] and Fig. 2.12 shows the vapor pressure of a number of liquids as a function of droplet radius.[41]

When two particles with different radii, assuming $R_1 >> R_2$, put into a solvent, each particle will develop an equilibrium with the surrounding solvent. According to Eq. (2.16), solubility of the smaller particle will be larger than that of the larger particle. Consequently, there would be a net diffusion of solute from proximity of the small particle to proximity of the large particle. To maintain the equilibrium, solute will deposit onto the surface of the large particle, whereas the small particle has to continue dissolving so as to compensate the amount of solute diffused away. As a result, the small particle gets smaller, whereas the large particle gets larger. Figure 2.13 depicts such a process. This phenomenon is called Ostwald ripening, which occurs also in the forms of solid-state diffusion and of evaporation-condensation. Assuming there is no other change between two different particles, then the change of the chemical potential of an atom transferring from a spherical surface of radius R_1 to R_2 is given by:

$$\Delta\mu = 2\gamma\Omega\,(R_2^{-1} - R_1^{-1}). \tag{2.17}$$

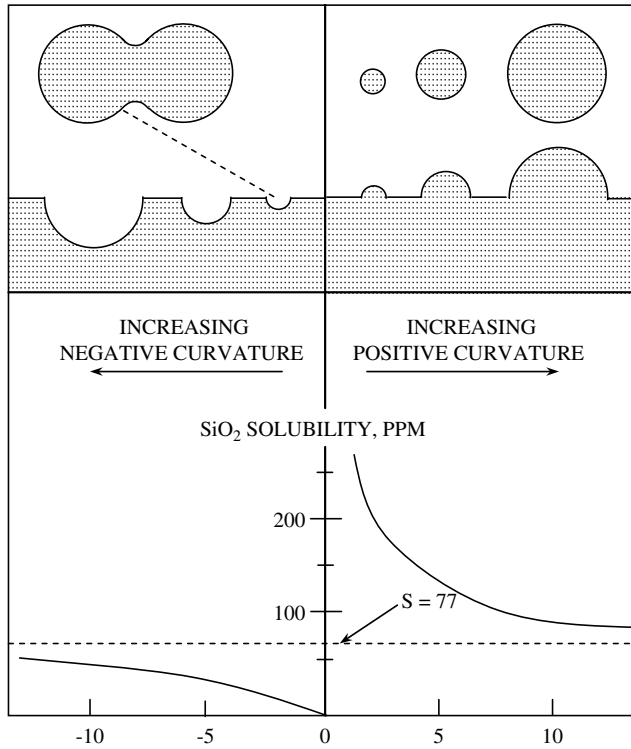

Figure 2.11. Variation in solubility of silica with radius of curvature of surface. The positive radii of curvature are shown in cross-section as particles and projections from a planar surface; negative radii are shown as depressions or holes in the surface, and in the crevice between two particles. [R.K. Iler, *The Chemistry of Silica*, Wiley, New York, 1979.]

This equation should not be confused with the Kelvin equation (Eq. (2.9)). Depending on the process and applications, Ostwald ripening can have either positive or negative influence on the resulting materials. Ostwald ripening can either widen or narrow the size distribution, depending on the control of the process conditions. In processing of many materials, Ostwald ripening is often not desirable. In sintering of polycrystalline materials, Ostwald ripening results in abnormal grain growth, leading to inhomogeneous microstructure and inferior mechanical properties of the products. Typically one or a few large grains grow at the

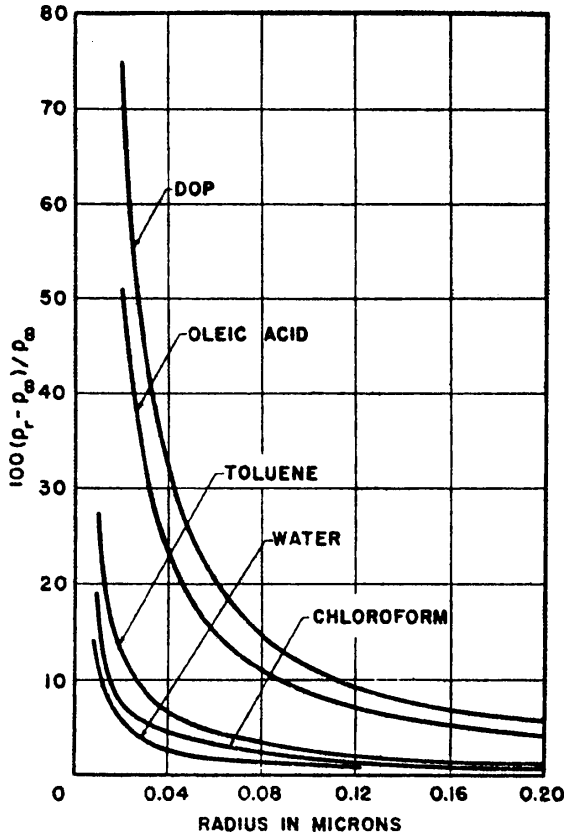

Figure 2.12. Vapor pressure of a number of liquids as a function of droplet radius. [V.K. La Mer and R. Gruen, *Trans. Faraday Soc*. **48**, 410 (1952).]

expense of a number of surrounding small grains, resulting in inhomogeneous microstructure. However, Ostwald ripening has been explored in the synthesis of nanoparticles. More specifically, Ostwald ripening has been used to narrow the size distribution of nanoparticles by eliminating small particles. The situation here is very different. Many relatively large particles grow at the expense of a relatively small number of smaller particles. The result is the elimination of smaller particles, and thus the size distribution of nanoparticles becomes narrower. Ostwald ripening can be promoted by varying processing temperatures. In the synthesis of

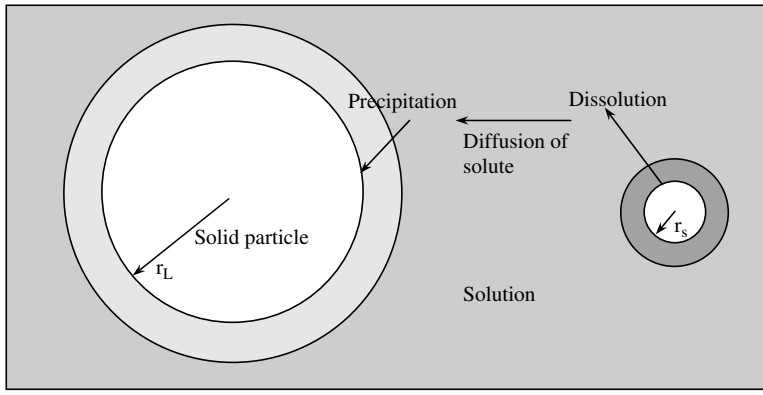

Figure 2.13. Schematic illustrating the Ostwald ripening processing. Smaller particle has a larger solubility or vapor pressure due to its larger curvature, whereas the larger particle possesses a smaller solubility or vapor pressure. To maintain the local concentration equilibrium, smaller particle would dissolve into the surrounding medium; solute at proximity of smaller particle diffuses away; solute at proximity of larger particle would deposit. The process would continue till disappearance of the smaller particle.

nanoparticles from solution, after the initial nucleation and subsequent growth, temperature is raised, and thus the solubility of solid in solvent increases to promote Ostwald ripening. As a result, the concentration of solid in solvent falls below the equilibrium solubility of small nanoparticles, and the small particles dissolve into the solvent. As dissolution of a nanoparticle proceeds, the nanoparticle becomes smaller and has higher solubility. It is clear that once a nanoparticle starts dissolving into the solvent, the dissolution process stops only when the nanoparticle dissolved completely. On the other hand, the concentration of solid in solvent is still higher than the equilibrium solubility of larger particles and, thus, these large particles would continue to grow. Such a growth process would stop when the concentration of solid in the solvent equals to the equilibrium solubility of these relatively large nanoparticles.

The reduction of overall surface energy is the driving force for the surface restructuring, formation of faceted crystals, sintering and Ostwald ripening. These are the reduction mechanisms for individual surface, individual nanostructures, and the overall system. The system can have another mechanism to reduce the overall surface energy, in addition to sintering

and Ostwald ripening. This is agglomeration. When small nanostructures form agglomerates, it is very difficult to disperse them. In nanostructure fabrication and processing, it is very important to overcome the huge total surface energy to create the desired nanostructures. It is equally important to prevent the nanostructures from agglomeration. As the dimension of nanostructured materials reduces, van der Waals attraction force between nanostructured materials becomes increasingly important. Without appropriate stabilization mechanisms applied, the nanostructured materials are most likely and readily to form agglomerates. The following sections are devoted to the stabilization mechanisms for the prevention of agglomeration of individual nanostructures. Although the discussion will be focused mainly on nanoparticles, the same principles are applicable to other nanostructures, such as nanorods and nanofibrils. There are two major stabilization mechanisms widely used: electrostatic stabilization and steric stabilization. Two mechanisms have some distinct differences. For example, a system using electrostatic stabilization is kinetic stable, whereas steric stabilization makes the system thermodynamically stable.

2.4. Electrostatic Stabilization

2.4.1. *Surface charge density*

When a solid emerges in a polar solvent or an electrolyte solution, a surface charge will be developed through one or more of the following mechanisms:

(1) Preferential adsorption of ions
(2) Dissociation of surface charged species
(3) Isomorphic substitution of ions
(4) Accumulation or depletion of electrons at the surface
(5) Physical adsorption of charged species onto the surface.

For a given solid surface in a given liquid medium, a fixed surface electrical charge density or electrode potential, E, will be established, which is given by the Nernst equation:

$$E = E_0 + \frac{RT}{n_i F} \ln(a_1), \tag{2.18}$$

where E_0 is the standard electrode potential when the concentration of ions is unity, n_i is the valence state of ions, R is the gas constant and T is temperature, and F is the Faraday's constant. Equation (2.18) clearly indicates that the surface potential of a solid varies with the concentration of the ions in the surrounding solution, and can be either positive or negative. Electrochemistry of metals will be discussed further in Sec. 4.3.1 in Chapter 4. The focus of the discussion here will be on nonconductive materials or dielectrics, more specifically on oxides.

The surface charge in oxides is mainly derived from preferential dissolution or deposition of ions. Ions adsorbed on the solid surface determine the surface charge, and thus are referred to as charge determining ions, also known as co-ions or coions. In the oxide systems, typical charge determining ions are protons and hydroxyl groups and their concentrations are described by pH ($pH = -\log [H^+]$). As the concentration of charge determining ions varies, the surface charge density changes from positive to negative or vice versa. The concentration of charge determining ions corresponding to a neutral or zero-charged surface is defined as a point of zero charge (*p.z.c.*) or zero-point charge (*z.p.c.*). For the sake of clarity and consistence, in the rest of this book, we will use the term of point of zero charge or *p.z.c.* only. Table 2.2 gives a list of some *p.z.c.* values of selected oxides.[43–45] At $pH > p.z.c.$, the oxide surface is negatively charged, since the surface is covered with hydroxyl groups, OH^-, which is the electrical determining ion. At $pH < p.z.c.$, H^+ is the charge determining ions and the surface is positively charged. The surface charge density or surface potential, E in volt, can then be simply related to the pH and the Nernst equation (Eq. (2.18)) can be written as[45]:

$$E = 2.303\, R_g T\, \frac{(p.z.c.) - pH}{F}. \tag{2.19}$$

At room temperature, the above equation can be further simplified:

$$E \approx 0.06[(p.z.c.) - pH]. \tag{2.20}$$

2.4.2. *Electric potential at the proximity of solid surface*

When a surface charge density of a solid surface is established, there will be an electrostatic force between the solid surface and the charged species

Table 2.2. A list of *z.p.c.* of some common oxides in water.[45]

Solids	*z.p.c.*
WO_3	0.5
V_2O_5	1–2
δ-MnO_2	1.5
β-MnO_2	7.3
SiO_2	2.5
SiO_2 (quartz)	3.7
TiO_2	6
TiO_2 (calcined)	3.2
SnO_2	4.5
Al-O-Si	6
ZrO_2	6.7
FeOOH	6.7
Fe_2O_3	8.6
ZnO	8
Cr_2O_3	8.4
Al_2O_3	9
MgO	12

in the proximity to segregate positive and negatively charged species. However, there also exist Brownian motion and entropic force, which homogenize the distribution of various species in the solution. In the solution, there always exist both surface charge determining ions and counter-ions, which have opposite charge of the determining ions. Although charge neutrality is maintained in a system, distributions of charge determining ions and counter-ions in the proximity of the solid surface are inhomogeneous and very different. The distributions of both ions are mainly controlled by a combination of the following forces:

(1) Coulombic force or electrostatic force
(2) Entropic force or dispersion
(3) Brownian motion.

The combined result is that the concentration of counter-ions is the highest near the solid surface and decreases as the distance from the surface

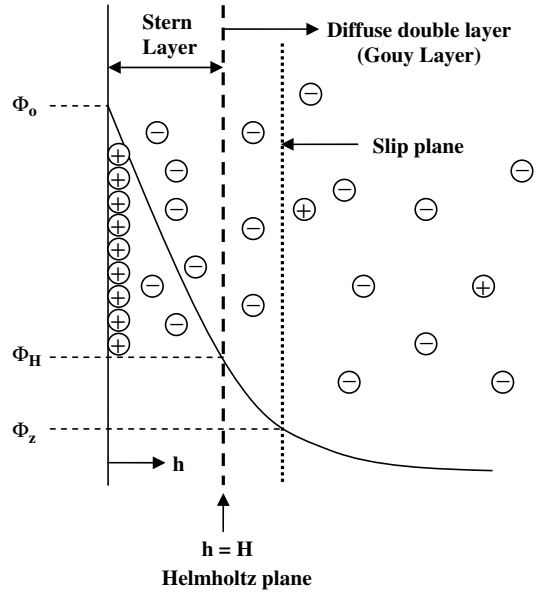

Figure 2.14. Schematic illustrating electrical double layer structure and the electric potential near the solid surface with both Stern and Gouy layers indicated. Surface charge is assumed to be positive.

increases, whereas the concentration of determining ions changes in the opposite manner. assuming surface charge is positive. Such inhomogeneous distributions of ions in the proximity of the solid surface lead to the formation of so-called double layer structure, which is schematically illustrated in Fig. 2.14. The double layer consists of two layers, Stern layer and Gouy layer (also called diffuse double layer), and the two layers are separated by the Helmholtz plane.[46] Between the solid surface and the Helmholtz plane is the Stern layer, where the electric potential drops linearly through the tightly bound layer of solvent and counter-ions. Beyond the Helmholtz plane until the counter-ions reach average concentration in the solvent is the Gouy layer or diffuse double layer. In the Gouy layer, the counter-ions diffuse freely and the electric potential does not reduce linearly. The electric potential drops approximately following:

$$E \propto e^{-\kappa(h-H)}, \tag{2.21}$$

where $h \geq H$, which is the thickness of the Stern layer, $1/\kappa$ is known as the Debye–Hückel screening strength and is also used to describe the thickness of double layer, and κ is given by:

$$\kappa = \left\{ \frac{F^2 \sum_i C_i Z_i^2}{\varepsilon \varepsilon_0 R_g T} \right\}^{1/2} \tag{2.22}$$

where F is Faraday's constant, ε_0 is the permittivity of vacuum, ε is the dielectric constant of the solvent, and C_i and Z_i are the concentration and valence of the counter-ions of type i. This equation clearly indicates that the electric potential at the proximity of solid surface decreases with increased concentration and valence state of counter-ions, and increases with an increased dielectric constant of the solvent exponentially. Higher concentration and valence state of counter-ions would result in a reduced thickness of both Stern layer and Gouy layer.[47,48] In theory, the Gouy diffusion layer would end at a point where the electric potential reaches zero, which would be the case only when the distance from the solid surface is infinite. However, in practice, double layer thickness is typically of approximately 10 nm or larger.

Although the above discussion has been focused on a flat solid surface in an electrolyte solution, the concepts are applicable to curved surfaces as well, assuming that the surface is smooth and thus the surface charge is distributed uniformly. For a smooth curved surface, the surface charge density is constant, so that the electric potential in the surrounding solution can be described using Eqs. (2.21) and (2.22). Such assumptions are certainly valid for spherical particles, when particles are dispersed in an electrolyte solution and the distance between any two particles are large enough so that the charge distribution on particle surface is not influenced by other particles. Interactions between particles are complex. One of the interactions between particles is directly associated with the surface charge and the electric potential adjacent to the interface. The electrostatic repulsion between two particles arises from the electric surface charges, which are attenuated to a varied extent by the double layers. When two particles are far apart, there will be no overlap of two double layers and electrostatic repulsion between two particles is zero. However, when two particles approach one another, double layer overlaps and a repulsive force develops. An

electrostatic repulsion between two equally sized spherical particles is given by[46]:

$$\Phi_R = 2\pi\varepsilon_r\varepsilon_0 r\, E^2 \exp(-\kappa S). \tag{2.23}$$

2.4.3. *Van der Waals attraction potential*

When particles are small, typically in micrometers or less, and are dispersed in a solvent, van der Waals attraction force and Brownian motion play important roles, whereas the influence of gravity becomes negligible. For the sake of simplicity, we will refer these particles to as nanoparticles, though particles in micrometer size behave the same and are also included in the discussion here. Furthermore, we will limit our discussion on spherical nanoparticles. Van der Waals force is a weak force and becomes significant only at a very short distance. Brownian motion ensures the nanoparticles colliding with each other all the time. The combination of van der Waals attraction force and Brownian motion would result in the formation of agglomeration of the nanoparticles.

Van der Waals interaction between two nanoparticles is the sum of the molecular interaction for all pair of molecules composed of one molecule in each particle, as well as to all pairs of molecules with one molecule in a particle and one in the surrounding medium such as solvent. Integration of all the van der Waals interactions between two molecules over two spherical particles of radius, r, separated by a distance, S, as illustrated in Fig. 2.15 gives the total interaction energy or attraction potential[46]:

$$\Phi_A = -\frac{A}{6}\left\{\frac{2r^2}{S^2+4rS} + \frac{2r^2}{S^2+4rS+4r^2} + \ln\left(\frac{S^2+4rS}{S^2+4rS+4r^2}\right)\right\}, \tag{2.24}$$

where the negative sign represents the attraction nature of the interaction between two particles, and A is a positive constant termed the Hamaker constant, which has a magnitude on the order of 10^{-19} to 10^{-20} J, and depends on the polarization properties of the molecules in the two particles and in the medium which separates them. Table 2.3 listed some Hamaker constants for a few common materials.[45] Equation (2.24) can be simplified under various boundary conditions. For example, when the

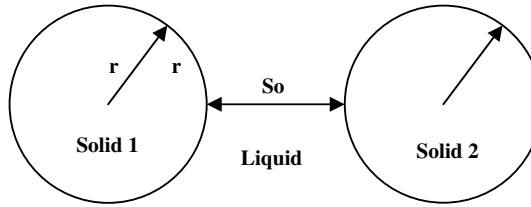

Figure 2.15. Pair of particles used to derive the van der Waals interaction.

Table 2.3. Hamaker constants for some common materials.[45]

Materials	A_i (10^{-20} J)
Metals	16.2–45.5
Gold	45.3
Oxides	10.5–15.5
Al_2O_3	15.4
MgO	10.5
SiO_2 (fused)	6.5
SiO_2 (quartz)	8.8
Ionic crystals	6.3–15.3
CaF_2	7.2
Calcite	10.1
Polymers	6.15–6.6
Polyvinyl chloride	10.82
Polyethylene oxide	7.51
Water	4.35
Acetone	4.20
Carbon tetrachloride	4.78
Chlorobenzene	5.89
Ethyl acetate	4.17
Hexane	4.32
Toluene	5.40

separation distance between two equal-sized spherical particles are significantly smaller than the particle radius, i.e., $S/r << 1$, the simplest expression of the van der Waals attraction could be obtained:

$$\Phi_A = \frac{-Ar}{12S}. \tag{2.25}$$

Table 2.4. Simple formulas for the van der Waals attraction between two particles.[46]

Particles	Φ_A
Two spheres of equal radius, r*	$-Ar/12S$
Two spheres of unequal radii, r_1 and r_2*	$-Ar_1 r_2/6S(r_1 + r_2)$
Two parallel plates with thickness of δ, interaction per unit area	$-A/12\pi[S^{-2} + (2\delta + S)^{-2} + (\delta + S)^{-2}]$
Two blocks, interaction per unit area	$-A/12\pi S^2$

*r, r_1 and $r_2 >> S$.

Other simplified expressions of the van der Waals attraction potential are summarized in Table 2.4.[46] From this table, it is noticed that the van der Waals attraction potential between two particles are different from that between two flat surfaces. Furthermore, it should be noted that the interaction between two molecules are significantly different from that between two particles. Van der Waals interaction energy between two molecules can be simply represented by:

$$\Phi_A \propto - S^{-6}. \tag{2.26}$$

Although the nature of the attraction energy between two particles is the same as that between two molecules, integration of all the interaction between molecules from two particles and from medium results in a totally different dependence of force on distance. The attraction force between two particles decay much slowly and extends over distances of nanometers. As a result, a barrier potential must be developed to prevent agglomeration. Two methods are widely applied to prevent agglomeration of particles: electrostatic repulsion and steric exclusion.

2.4.4. *Interactions between two particles: DLVO theory*

The total interaction between two particles, which are electrostatic stabilized, is the combination of van der Waals attraction and electrostatic repulsion:

$$\Phi = \Phi_A + \Phi_R. \tag{2.27}$$

The electrostatic stabilization of particles in a suspension is successfully described by the DLVO theory, named after Derjaguin, Landau, Verwey, and Overbeek. The interaction between two particles in a suspension is considered to the combination of van der Waals attraction potential and the electric repulsion potential. There are some important assumptions in the DLVO theory:

(1) Infinite flat solid surface
(2) Uniform surface charge density
(3) No redistribution of surface charge, i.e., the surface electric potential remains constant
(4) No change of concentration profiles of both counter-ions and surface charge determining ions, i.e., the electric potential remains unchanged, and
(5) Solvent exerts influences via dielectric constant only, i.e., no chemical reactions between the particles and solvent.

It is very clear that some of the assumptions are far from the real picture of two particles dispersed in a suspension. For example, the surface of particles is not infinitely flat, and the surface charge density is most likely to change when two charged particles get very close to each other. However, in spite of the assumptions, the DLVO theory works very well in explaining the interactions between two approaching particles, which are electrically charged, and thus is widely accepted in the research community of colloidal science.

Figure 2.16 shows the van der Waals attraction potential, electric repulsion potential, and the combination of the two opposite potentials as a function of distance from the surface of a spherical particle.[47] At a distance far from the solid surface, both van der Waals attraction potential and electrostatic repulsion potential reduce to zero. Near the surface is a deep minimum in the potential energy produced by the van der Waals attraction. A maximum is located a little farther away from the surface, as the electric repulsion potential dominates the van der Waals attraction potential. The maximum is also known as repulsive barrier. If the barrier is greater than ~10 kT, where k is Boltzmann constant, the collisions of two particles produced by Brownian motion will not overcome the barrier and agglomeration will not occur. Since the electric potential is dependent

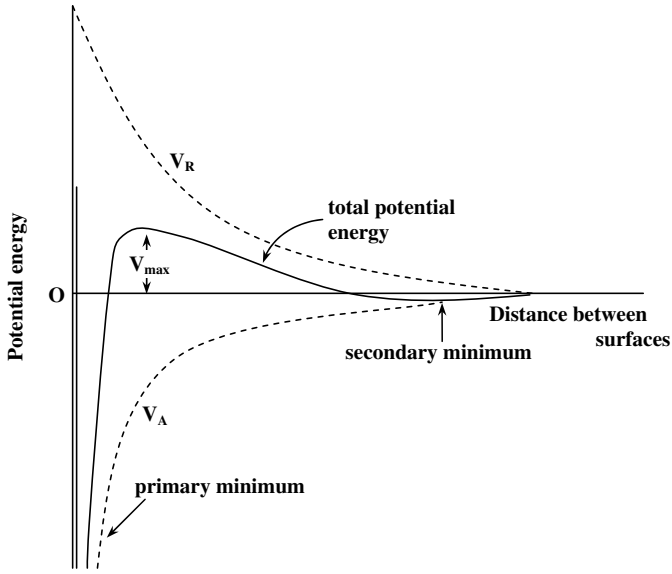

Figure 2.16. Schematic of DLVO potential: V_A = attractive van der Waals potential, V_R = repulsive electrostatic potential.

on the concentration and valence state of counter-ions as given in Eqs. (2.21) and (2.22) and the van der Waals attraction potential is almost independent of the concentration and valence state of counter-ions, the overall potential is strongly influenced by the concentration and valence state of counter-ions. An increase in concentration and valence state of counter-ions results in a faster decay of the electric potential as schematically illustrated in Fig. 2.17.[49] As a result, the repulsive barrier is reduced and its position is pushed towards the particle surface. The secondary minimum in Fig. 2.17 is not necessary to exist in all situations, and it is present only when the concentration of counter-ions is higher enough. If secondary minimum is established, particles likely associate with each other, which is known as flocculation.

When two particles are far apart or the distance between the surfaces of two particles is larger than the combined thickness of two electric double layers of two particles, there would be no overlap of diffusion double layers, and thus there would be no interaction between two particles

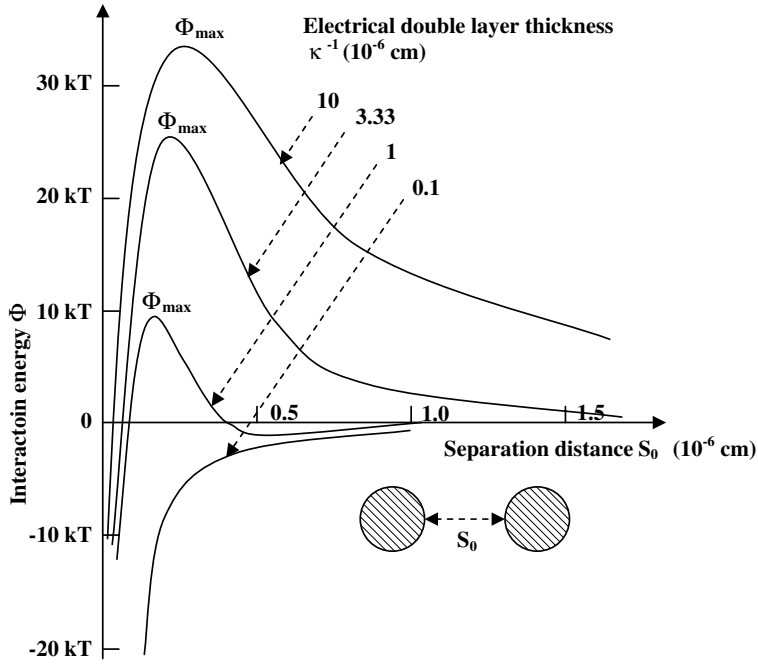

Figure 2.17. Variation of the total interaction energy Φ between two spherical particles, as a function of the closest separation distance S_0 between their surfaces, for different double layer thickness κ^{-1} obtained with different monovalent electrolyte concentrations. The electrolyte concentration is $C\,(\text{mol}\cdot\text{L}^{-1}) = 10^{-15}\kappa^2\,(\text{cm}^{-1})$. [J.T.G. Overbeek, *J. Coll. Interf. Sci.* **58**, 408 (1977).]

(Fig. 2.18(a)). However, when two particles move closer and the two electric double layers overlaps, a repulsion force is developed. As the distance reduces, the repulsion increases and reaches the maximum when the distance between two particle surfaces equals to the distance between the repulsive barrier and the surface (Fig. 2.18(b)). Such a repulsion force can be understood in two ways. One is that the repulsion derives from the overlap of electric potentials of two particles. It should be noted that the repulsion is not directly due to the surface charge on solid particles, instead it is the interaction between two double layers. The other is the osmotic flow. When two particles approach one another, the concentrations of ions between two particles where two double layers overlap,

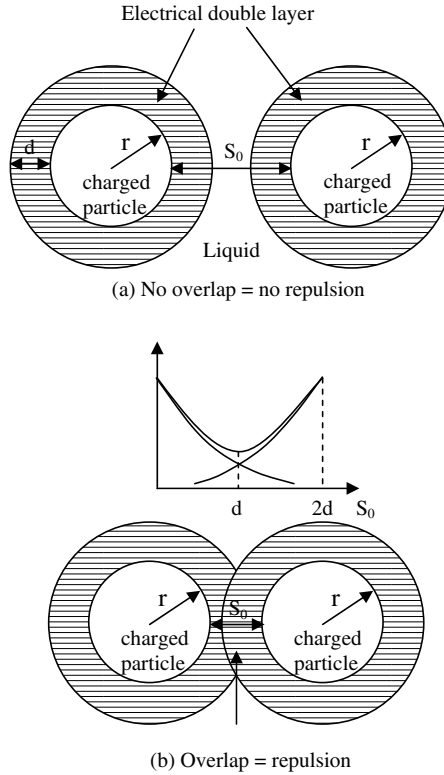

Figure 2.18. Schematic illustrating the conditions for the occurrence of electrostatic repulsion between two particles.

increase significantly, since each double layer would retain its original concentration profile. As a result, the original equilibrium concentration profiles of counter-ions and surface charge determining ions are destroyed. To restore the original equilibrium concentration profiles, more solvent needs to flow into the region where the two double layers overlap. Such an osmotic flow of solvent effectively repels two particles apart, and the osmotic force disappears only when the distance between the two particles equals to or becomes larger than the sum of the thickness of the two double layers.

Although many important assumptions of the DLVO theory are not satisfied in the really colloidal systems, in which small particles dispersed

in a diffusive medium, the DLVO theory is still valid and has been widely applied in practice, as far as the following conditions are met:

(1) Dispersion is very dilute, so that the charge density and distribution on each particle surface and the electric potential in the proximity next to each particle surface are not interfered by other particles
(2) No other force is present besides van der Waals force and electrostatic potential, i.e., the gravity is negligible or the particle is significantly small, and there exist no other forces, such as magnetic field
(3) Geometry of particles is relatively simple, so that the surface properties are the same over the entire particle surface, and, thus surface charge density and distribution as well as the electric potential in the surrounding medium are the same
(4) The double layer is purely diffusive, so that the distributions of counter-ions and charge determining ions are determined by all three forces: electrostatic force, entropic dispersion, and Brownian motion.

However, it should be noted that electrostatic stabilization is limited by the following facts:

(1) Electrostatic stabilization is a kinetic stabilization method
(2) It is only applicable to dilute systems
(3) It is not applicable to electrolyte sensitive systems
(4) It is almost not possible to redisperse the agglomerated particles
(5) It is difficult to apply to multiple phase systems, since in a given condition, different solids develop different surface charge and electric potential.

2.5. Steric Stabilization

Steric stabilization, also called polymeric stabilization is a method widely used in stabilization of colloidal dispersions and thoroughly discussed in literature,[50–52] though it is less well-understood as compared with electrostatic stabilization method. Polymeric stabilization does offer several advantages over electrostatic stabilization:

(1) It is a thermodynamic method, so that the particles are always redispersible
(2) A very high concentration can be accommodated, and the dispersion medium can be completely depleted

(3) It is not electrolyte sensitive
(4) It is suitable to multiple phase systems.

In this section, we will briefly summarize the essential concepts of polymeric stabilization. Compared to electrostatic stabilization mechanism, polymeric stabilization offers an additional advantage in the synthesis of nanoparticles, particularly when narrow size distribution is required. Polymer layer adsorbed on the surface of nanoparticles serve as a diffusion barrier to the growth species, resulting in a diffusion-limited growth in the subsequent growth of nuclei. As will be discussed in detail in the next chapter, diffusion-limited growth would reduce the size distribution of the initial nuclei, leading to monosized nanoparticles. The dual functionalities of polymeric layer on the surface of nanoparticles explain the fact that steric stabilization is widely used in the synthesis of nanoparticles.

2.5.1. *Solvent and polymer*

Solvents can be grouped into aqueous solvent, which is water, H_2O, and nonaqueous solvents or organic solvents. Solvents can also been categorized into protic solvent, which can exchange protons and examples of which include: methanol, CH_3OH, and ethanol, C_2H_5OH, and aprotic solvent, which cannot exchange protons, such as benzene, C_6H_6. Table 2.5 gives some examples of typical protic and aprotic solvents.[53]

Not all polymers are dissolvable into solvents and those nonsolvable polymers will not be discussed in this chapter, since they cannot be used for the steric stabilization. When a solvable polymer dissolves into a solvent, polymer interacts with solvent. Such interaction varies with system as well as temperature. When polymer in a solvent tends to expand to reduce the overall Gibbs free energy of the system, such a solvent is called a "good solvent". When polymer in a solvent tends to coil up or collapse to reduce the Gibbs free energy, the solvent is considered to be a "poor solvent".

For a given system, i.e., a given polymer in a given solvent, whether the solvent is a "good" or "poor" solvent is dependent on the temperature. At high temperatures, polymer expands, whereas at low temperatures,

Table 2.5. List of some solvents with their dielectric constants.

Solvent	Formula	Dielectric constant	Type
Acetone	C_3H_6O	20.7	Aprotic
Acetic acid	$C_2H_4O_2$	6.2	Protic
Ammonia	NH_3	16.9	Protic
Benzene	C_6H_6	2.3	Aprotic
Chloroform	$CHCl_3$	4.8	Aprotic
Dimethylsulfoxide	$(CH_3)_2SO$	45	Aprotic
Dioxanne	$C_4H_8O_2$	2.2	Aprotic
Water	H_2O	78.5	Protic
Methanol	CH_3OH	32.6	Protic
Ethanol	C_2H_5OH	24.3	Protic
Formamide	CH_3ON	110.0	Protic
Dimethylformamide	C_3H_7NO	36.7	Aprotic
Nitrobenzene	$C_6H_5NO_2$	34.8	Aprotic
Tetrahydrofuran	C_4H_8O	7.3	Aprotic
Carbon tetrachloride	CCl_4	2.2	Aprotic
Diethyl ether	$C_4H_{10}O$	4.3	Aprotic
Pyridine	C_5H_5N	14.2	Aprotic

polymer collapses. The temperature, at which a poor solvent transfers to a good solvent, is the Flory–Huggins theta temperature, or simply the θ temperature. At $T = \theta$, the solvent is considered to be at the theta state, at which the Gibbs free energy does not change whether polymer expands or collapses.

Depending on the interaction between polymer and solid surface, polymer can be grouped into:

(1) Anchored polymer, which irreversibly binds to solid surface by one end only, and typically are diblock polymer (Fig. 2.19(a))
(2) Adsorbing polymer, which adsorbs weakly at random points along the polymer backbone (Fig. 2.19(b))
(3) Nonadsorbing polymers, which does not attach to solid surface and thus does not contribute to polymer stabilization, and thus is not discussed further in this chapter.

The interaction between polymer and solid surface are limited to adsorption of polymer molecules onto the surface of solid. The adsorption can be

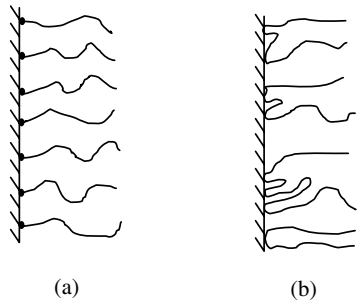

Figure 2.19. Schematic of different polymers according to the interaction between polymers and solid surface: (a) anchored polymer and (b) absorbing polymer.

either by forming chemical bonds between surface ions or atoms on the solid and polymer molecules or by weak physical adsorption. Furthermore, there is no restriction whether one or multiple bonds formed between solid and polymer. No other interactions such as chemical reactions or further polymerization between polymer and solvent or between polymers are considered for the current discussion.

2.5.2. *Interactions between polymer layers*

First let us consider two solid particles covered with terminally anchored polymers as schematically illustrated in Fig. 2.20(a). When two particles approach one another, the attached polymers interact only when the separation distance, H, between the surfaces of two particles is less than twice the thickness, L, of polymer layers. Beyond this distance, there is no interaction between two particles and their polymer layers on surfaces. However, when the distance reduces to less than $2L$, but still is larger than, L, there will be interactions between solvent and polymer and between two polymer layers. But there is no direct interaction between the polymer layer of one particle and the solid surface of opposite particle. In a good solvent, in which polymer expands, if the coverage of polymer on the solid surface is not complete, particularly less than 50% coverage, when the concentration of polymer in the solvent is insufficient, two polymer layers tend to interpenetrate so as to reduce the available space between polymers.

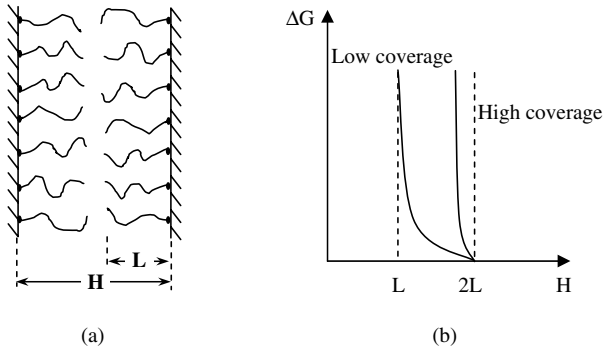

Figure 2.20. Schematic of interactions between polymer layers: (a) the schematic of two approaching polymer layers and (b) the Gibb's free energy as a function of the distance between two particles.

Such an interpenetration of two polymer layers of two approaching particles would result in a reduction of the freedom of polymers, which leads to a reduction of entropy, i.e., $\Delta S < 0$. As a result, the Gibbs free energy of the system would increase, assuming the change of enthalpy due to the interpenetration of two polymer layers negligible, i.e., $\Delta H \approx 0$, according to:

$$\Delta G = \Delta H - T\Delta S > 0. \tag{2.28}$$

So two particles repel one another and the distance between two particles must be equal to or larger than the twice the thickness of polymer layers. When the coverage of polymer is high, particularly approaching 100%, there would be no interpenetration. As a result, the two polymer layers will be compressed, leading to the coil up of polymers in both layers. The overall Gibbs free energy increases, and repels two particles apart. When the distance between the surfaces of two particles is less than the thickness of polymer layers, a further reduction of the distance would force polymers to coil up and result in an increase in the Gibbs' free energy. Figure 2.20(b) sketches the Gibbs free energy as a function of the distance between two particles, and shows that the overall energy is always positive and increases with a decreasing distance when H is smaller than $2L$.

The situation is rather different in a poor solvent, with a low coverage of polymer on the solid surface. With a low coverage, when the distance between two particles is less than twice the thickness of polymer layers but larger than the thickness of single polymer layer, i.e., $L < H < 2L$, polymers adsorbed onto the surface of one particle surface tend to penetrate into the polymer layer of the approach particle. Such interpenetration of two polymer layers will promote further coil up of polymers, and result in a reduction of the overall Gibbs free energy. Two particles tend to associate with one another. However, with a high coverage, similar to polymer in a good solvent, there would be no penetration and the reduction in distance results in a compressive force, leading to an increase in the overall free energy. When the distance between two particles is less than the thickness of the polymer layer, a reduction in distance always produces a repulsive force and an increase in the overall Gibbs free energy. Figure 2.21 summarizes the dependence of free energy as a function of distance between two particles. Regardless the difference in coverage and solvent, two particles covered with polymer layers are prevented from agglomeration by the space exclusion or steric stabilization.

Next, let us look at the adsorbing polymers. The situation of adsorbing polymers is more complicated due to the following two reasons. First, polymer originally attached to the solid surface of one particle may

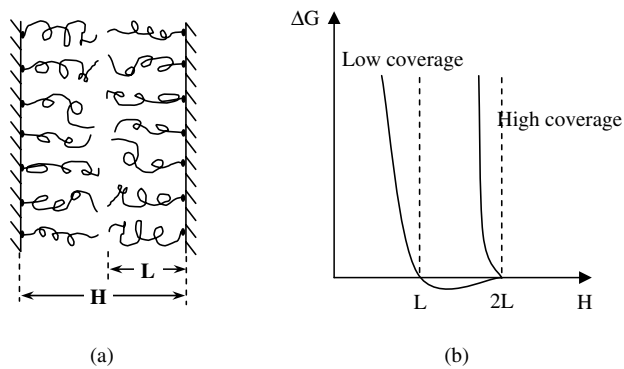

Figure 2.21. Schematic of interactions between polymer layers: (a) the schematic of two approaching polymer layers and (b) the Gibb's free energy as a function of the distance between two particles.

interact with and adsorb onto other particle surface, and thus form bridges between two particles, when two particles approach to a sufficiently close distance between each other. Second, given sufficient time, attached polymer can desorb from the surface and migrate out of the polymer layer.

When polymer has a strong adsorption and forms a full coverage, interaction between two polymer layers produces a purely repulsive force and results in an increased free energy, when the distance between two particles reduces below twice the thickness of polymer layer. This is the same as that of anchored polymer at full coverage. When only a partial coverage is achieved, the nature of solvent can have a significant influence on the interaction between two particles. In a good solvent, two partially covered polymer layers interpenetrate into each other, resulting in a reduced space and more ordered polymer arrangement. As a result, the entropy reduces and the Gibbs free energy increases. However, in a poor solvent, interpenetration promotes further coil up of polymers, leads to increased entropy, and thus results in a reduced free energy. This interaction force of adsorbing polymer layers in a poor solvent is very similar to that of anchored polymer layers with partial in poor solvent; however, the process involved is significantly different due to multiple adsorption sites at both surfaces. It is always the case that a repulsive force develops and repels two particles away from each other, when the distance is less than the thickness of polymer layer.

The physical basis for the steric stabilization is (1) a volume restriction effect arises from the decrease in possible configurations in the region

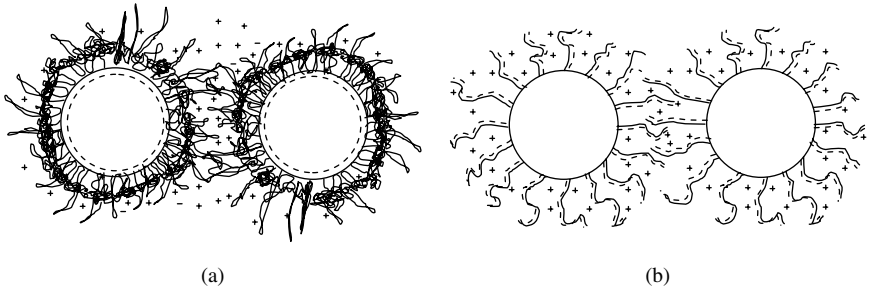

Figure 2.22. Schematic representation of electrosteric stabilization: (a) charged particles with nonionic polymers and (b) polyelectrolytes attached to uncharged particles.

between the two surfaces when two particles approach one another, and (2) an osmotic effect due to the relatively high concentration of adsorbed polymeric molecules in the region between the two particles.

2.5.3. *Mixed steric and electric interactions*

Steric stabilization can be combined with electrostatic stabilization, which is also referred to as electrosteric stabilization and is sketched in Fig. 2.22.[50] When polymers attached to a charge particle surface, a polymer layer would develop as discussed above. In addition, an electric potential adjacent to the solid surface would retain. When two particles approach each other, both electrostatic repulsion and steric restriction would prevent agglomeration.

2.6. Summary

This chapter has discussed the origins of the surface energy of solids, the various mechanisms for a material to reduce its surface energy, the influences of the surface curvature on the chemical potential, and the two mechanisms for the stabilization of nanoparticles from agglomeration. All the concepts and theories discussed in this chapter have been well-established in various surface science and materials fields. However, the impact of surface energy on nanostructures and nanomaterials would be far more significant, due to the huge surface area involved in nanosized materials. A good understanding of these fundamentals is not only important for the fabrication and processing of nanomaterials, it is equally important to the applications of nanomaterials.

References

1. C. Nützenadel, A. Züttel, D. Chartouni, G. Schmid, and L. Schlapbach, *Eur. Phys. J.* **D8**, 245 (2000).
2. A.W. Adamson and A.P. Gast, *Physical Chemistry of Surfaces*, 6th edn. John Wiley and Sons, New York, 1997.
3. A.N. Goldstein C.M. Echer, and A.P. Alivisatos, *Science* **256**, 1425 (1992).
4. M.A. Van Hove, W.H. Weinberg, and C.M. Chan, *Low-Energy Electron Diffraction*, Springer-Verlag, Berlin, 1986.

5. M.W. Finnis and V. Heine, *J. Phys*. **F4**, L37 (1974).
6. U. Landman, R.N. Hill, and M. Mosteller, *Phys. Rev.* **B21**, 448 (1980).
7. D.L. Adams, H.B. Nielsen, J.N. Andersen, I. Stengsgaard, R. Friedenhans'l, and J.E. Sorensen, *Phys. Rev. Lett.* **49**, 669 (1982).
8. C.M. Chan, M.A. Van Hove, and E.D. Williams, *Surf. Sci.* **91**, 440 (1980).
9. M.A. Van Hove, R.J. Koestner, P.C. Stair, J.P. Birberian, L.L. Kesmodell, I. Bartos, and G.A. Somorjai, *Surf. Sci*. **103**, 189 (1981).
10. I.K. Robinson, Y. Kuk, and L.C. Feldman, *Phys. Rev.* **B29**, 4762 (1984).
11. R.M. Tromp, R.J. Hamers, and J.E. Demuth, *Phys. Rev.* **B34**, 5343 (1986).
12. G. Binnig, H. Rohrer, Ch. Gerber, and E. Weibel, *Phys. Rev. Lett.* **50**, 120 (1983).
13. R. Schlier and H. Farnsworth, *J. Chem. Phys.* **30**, 917 (1959).
14. R.M. Tromp, R.J. Hames, and J.E. Demuth, *Phys. Rev. Lett.* **55**, 1303 (1985).
15. R.M. Tromp, R.J. Hames, and J.E. Demuth, *Phys. Rev.* **B24**, 5343 (1986).
16. J.M. Jasinski, B.S. Meyerson, and B.A. Scott, *Annu. Rev. Phys. Chem.* **38**, 109 (1987).
17. M. McEllistrem, M. Allgeier, and J.J. Boland, *Science* **279**, 545 (1998).
18. Z. Zhang, F. Wu, and M.G. Lagally, *Annu. Rev. Mater. Sci.* **27**, 525 (1997).
19. T. Tsuno, T. Imai, Y. Nishibayashi, K. Hamada, and N. Fujimori, *Jpn. J. Appl. Phys.* **30**, 1063 (1991).
20. C.J. Davisson and L.H. Germer, *Phys. Rev.* **29**, 908 (1927).
21. K. Christmann, R.J. Behm, G. Ertl, M.A. Van Hove, and W.H. Weinberg, *J. Chem. Phys.* **70**, 4168 (1979).
22. H.D. Shih, F. Jona, D.W. Jepsen, and P.M. Marcus, *Surf. Sci.* **60**, 445 (1976).
23. J.M. MacLaren, J.B. Pendry, P.J. Rous, D.K. Saldin, G.A. Somorjai, M.A. Van Hove, and D.D. Vvedensky (eds.), *Surface Crystallography Information Service*, Reidel Publishing, Dordrecht, 1987.
24. C. Herring, *Structure and Properties of Solid Surfaces*, University of Chicago, Chicago, IL, 1952.
25. W.W. Mullins, *Metal Surfaces*: *Structure Energetics and Kinetics*, The American Society for Metals, Metals Park, OH, 1963.
26. E. Matijević, *Annu. Rev. Mater. Sci.* **15**, 483 (1985).
27. H.N.V. Temperley, *Proc. Cambridge Phil. Soc.* **48**, 683 (1952).
28. W.K. Burton and N. Cabrera, *Disc. Faraday Soc.* **5**, 33 (1949).
29. G.K. Teal, *IEEE Trans. Electron Dev.* **ED-23**, 621 (1976).

30. W. Zuhlehner and D. Huber, *Czochralski Grown Silicon*, in *Crystals* 8, Springer-Verlag, Berlin, 1982.
31. W.D. Kingery, H.W. Bowen, and D.R. Uhlmann, *Introduction to Ceramics*, 2nd edn., Wiley, New York, 1976.
32. J.S. Reed, *Introduction to Principles of Ceramic Processing*, Wiley, New York, 1988.
33. E.P. DeGarmo, J.T. Black, and R.A. Kohner, *Materials and Processes in Manufacturing*, Macmillan, New York, 1988.
34. A.W. Adamson, *Physical Chemistry of Surfaces*, Wiley, New York, 1976.
35. L.R. Fisher and J.N. Israelachvili, *J. Coll. Interf. Sci.* **80**, 528 (1981).
36. J.C. Melrose, *Langmuir* **5**, 290 (1989).
37. R.W. Vook, *Int. Met. Rev.* **27**, 209 (1982).
38. R.K. Iler, *The Chemistry of Silica: Solubility, Polymerization, Colloid and Surface Properties, and Biochemistry*, John Wiley and Sons, New York, 1979.
39. J.R. Sambles, L.M. Skinner, and N.D. Lisgarten, *Proc. R. Soc.* **A324**, 339 (1971).
40. N.D. Lisgarten, J.R. Sambles, and L.M. Skinner, *Contemp. Phys.* **12**, 575 (1971).
41. V.K. La Mer and R. Gruen, *Trans. Faraday Soc.* **48**, 410 (1952).
42. F. Piuz and J.-P. Borel, *Phys. Status Solidi* **A14**, 129 (1972).
43. R.J. Hunter, *Zeta Potential in Colloid Science*, Academic Press, New York, 1981.
44. G.A. Parks, *Chem. Rev.* **65**, 177 (1965).
45. A.C. Pierre, *Introduction to Sol–Gel Processing*, Kluwer, Norwell, MA, 1998.
46. P.C. Hiemenz, *Principles of Colloid and Surface Chemistry*, Marcel Dekker, New York, 1977.
47. G.D. Parfitt, in *Dispersion of Powders in Liquids with Special Reference to Pigments*, ed. G.D. Parfitt, Applied Science, London, p.1, 1981.
48. C.J. Brinker and G.W. Scherer, *Sol–Gel Science*: *The Physics and Chemistry of Sol–Gel Processing*, Academic Press, San Diego, CA, 1990.
49. J.T.G. Overbeek, *J. Coll. Interf. Sci.* **58**, 408 (1977).
50. D.H. Napper, *Polymeric Stabilization of Colloidal Dispersions*, Academic Press, New York, 1983.
51. W.B. Russel, D.A. Saville, and W.R. Schowalter, *Colloidal Dispersions*, Cambridge University Press, Cambridge, 1991.

52. P. Somasundaran, B. Markovic, S. Krishnakumar, and X. Yu, in *Handbook of Surface and Colloid Chemistry*, ed. K.S. Birdi, CRC Press, Boca Raton, FL, p. 559, 1997.
53. J.J. Lagowski, *The Chemistry of Non-Aqueous Systems*, Vols. 1–4, Academic Press, New York, 1965, 1967, 1970, 1976.